

Selective Interaction of Lower Rim Calix[4]arene Derivatives and Bivalent Cations in Solution. Crystallographic Evidence of the Versatile Behavior of Acetonitrile in Lead(II) and Cadmium(II) Complexes

Angela F. Danil de Namor,^{*,†} Samir Chahine,[†] Dorota Kowalska,[†]
Eduardo E. Castellano,[‡] and Oscar E. Piro[§]

Contribution from the Laboratory of Thermochemistry, Department of Chemistry, University of Surrey, Guildford, Surrey GU2 7XH, UK, Instituto de Física de São Carlos, Universidade de São Paulo, C. P. 369, 13560 São Carlos (SP), Brazil, and Departamento de Física, Facultad de Ciencias Exactas, Universidad Nacional de La Plata and Instituto IFLP (CONICET – UNLP), C. C. 67, 1900 La Plata, Argentina

Received May 31, 2002

Abstract: The interaction of lower rim calix(4)arene derivatives containing ester (**1**) and ketone (**2**) functional groups and bivalent (alkaline-earth, transition- and heavy-metal) cations has been investigated in various solvents (methanol, *N,N*-dimethylformamide, acetonitrile, and benzonitrile). Thus, ¹H NMR studies in CD₃-OD, C₃D₇NO, and CD₃CN show that the interaction of these ligands with bivalent cations (Mg²⁺, Ca²⁺, Sr²⁺, Ba²⁺, Hg²⁺, Pb²⁺, Cd²⁺) is only observed in CD₃CN. These findings are corroborated by conductance measurements in these solvents including benzonitrile, where changes upon the addition of the appropriate ligand (**1** or **2**) to the metal-ion salt only occur in acetonitrile. Thus, in this solvent, plots of molar conductance against the ligand/metal cation ratio reveal the formation of 1:1 complexes between these ligands and bivalent cations. Four metal-ion complex salts resulting from the interaction of **1** and **2** with cadmium and lead, respectively, were isolated and characterized by X-ray crystallography. All four structures show an acetonitrile molecule sitting in the hydrophobic cavity of the ligand. The mode of interaction of the neutral guest in the cadmium(II) complexes differs from each other and from that found in the lead(II) complexes and provides evidence of the versatile behavior of acetonitrile in binding processes involving calix(4)arene derivatives. The thermodynamics of complexation of these ligands and bivalent cations in acetonitrile is reported. Thus, the selective behavior of **1** and **2** for bivalent cations is for the first time demonstrated. The role of acetonitrile in the complexation process in solution is discussed on the basis of ¹H NMR and X-ray crystallographic studies. It is suggested that the complexation of **1** and **2** with bivalent cations is likely to involve the ligand-solvent adducts rather than the free ligand. Plots of complexation Gibbs energies against the corresponding data for cation hydration show a selectivity peak which is explained in terms of the predominant role played by cation desolvation and ligand binding energy in complex formation involving metal cations and macrocycles in solution. A similar peak is found in terms of enthalpy suggesting that for most cations (except Mg²⁺) the selectivity is enthalpically controlled. The ligand effect on the complexation process is quantitatively assessed. Final conclusions are given highlighting the role of the solvent in complexation processes involving calix(4)arene derivatives and metal cations.

Introduction

Calixarenes (products of the base condensation reaction between *p*-substituted phenols and formaldehyde) and their lower and upper rim derivatives have found widespread applications.^{1–5}

The presence of a hydrophobic cavity (able to host neutral species) besides the hydrophilic one (able to interact with ionic species) confers outstanding properties to calix(4)arene derivatives in their “cone” conformation relative to macrocycles such as crown ethers⁶ and cryptands.⁷

Calix(4)arenes containing ester and ketone functional groups at the lower rim have shown pronounced selectivity for alkali-metal cations in different media, particularly acetonitrile.

* Address correspondence to this author. E-mail: a.danil-de-namor@surrey.ac.uk.

[†] University of Surrey.

[‡] Universidade de São Paulo.

[§] Universidad Nacional de La Plata and Instituto IFLP (CONICET – UNLP).

(1) Gutsche, C. D. *Calixarenes. Monographs in Supramolecular Chemistry*; Stoddart, J. F., Ed.; Royal Society of Chemistry: , 1989.

(2) *Calixarenes. A Versatile Class of Macrocyclic Compounds*; Vicens, J., Böhrer, V., Eds.; Kluwer Academic Publishers: Dordrecht, The Netherlands, 1991.

(3) *Calixarenes 50th Anniversary, Commemorative Volume*; Vicens, J., Asfari, Z., Harrowfield, J. M., Eds.; Kluwer Academic Publishers: Dordrecht, The Netherlands, 1994.

(4) Gutsche, C. D. *Calixarenes Revisited. Monographs in Supramolecular Chemistry*; Stoddart, J. F., Ed.; The Royal Society of Chemistry, 1998.

(5) *Calixarenes 2001*; Asfari, Z., Böhrer, V., Harrowfield, I. M., Vicens, J., Eds.; Kluwer Academic Publishers: Dordrecht, The Netherlands, 2001.

(6) Pedersen, C. J. *Angew. Chem., Int. Ed. Engl.* **1989**, *27*, 1923; Nobel Lecture.

(7) Lehn, J. M. *Angew. Chem., Int. Ed. Engl.* **1989**, *27*, 89; Nobel Lecture.

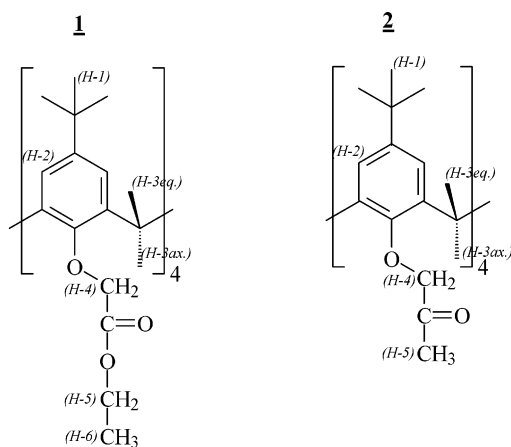


Figure 1. Tetraethylester *p*-*tert*-butyl calix[4]arene, **1**; and tetramethyl ketone *p*-*tert*-butyl calix[4]arene, **2**.

It is now well established from detailed experimental thermodynamics that, among cations, calix(4)arene esters and ketones show the highest selectivity for sodium in acetonitrile, methanol, and benzonitrile.^{8,9} However, there are no systematic studies on these ligands and bivalent cations in different media. Complex formations between calix(4)arene esters and ketones with alkaline-earth metal cations were only investigated in methanol, and these led to the conclusion that these ligands do not complex with these cations.⁹ However, ¹H NMR studies on calix(4)arene esters and ketones show considerable conformational changes with the solvent which may alter their capability to interact with metal cations.¹⁰ Therefore, it is of particular relevance to current studies to assess the medium effect on the complexation process involving calix(4)arene derivatives and bivalent cations.

We report here a detailed investigation on the complexation of the **1** and **2** (Figure 1) with alkaline-earth and transition- and heavy-metal cations in a wide variety of solvents (methanol, MeOH; *N,N*-dimethylformamide, DMF; dimethyl sulfoxide, Me₂SO; acetonitrile, MeCN; and benzonitrile, PhCN) using a variety of techniques such as ¹H NMR (to determine the active sites of interaction of the ligands), conductance measurements (to establish the complex composition and the speciations in solution), calorimetry (macro and micro) to derive the thermodynamics of complexation (stability constant, log *K*_s, hence standard Gibbs energy, Δ_cG°; enthalpy, Δ_cH°; and entropy, Δ_cS° of complexation). Stability constants are used to assess quantitatively the selective behavior of these ligands for one cation relative to another. The factors influencing the thermodynamics of complexation of these derivatives and bivalent cations are first discussed. The X-ray structures of the lead and the cadmium complexes of **1** and **2** with acetonitrile are reported.

Experimental Section

Chemicals. Lead(II) perchlorate trihydrate 98%, cadmium(II) perchlorate hydrate, mercury(II) perchlorate 98%, calcium(II) perchlorate hexahydrate, magnesium(II) perchlorate hexahydrate, 99%, barium(II)

perchlorate hydrate, strontium(II) perchlorate hydrate, cobalt perchlorate hexahydrate, and zinc perchlorate hexahydrate were all purchased from Aldrich Chemical Co. These were dried over P₄O₁₀ under vacuum for several days before use.

Tris(hydroxymethyl)aminomethane, ultrapure grade 99.9% from Aldrich was used without any further purification.

MeCN (Aldrich; HPLC-grade) was purified by refluxing the solvent in a nitrogen atmosphere and distilled over calcium hydride. The middle fraction of the distilled solvent was used.¹¹

DMF (Fisher; HPLC-grade) was dried over 3 Å molecular sieves (which had been dried in an oven at 300°C overnight) for 72 h followed by distillation under reduced pressure.¹²

Me₂SO (Fisher, HPLC-grade) was dried overnight over calcium sulfate, filtered, and then fractionally distilled over calcium hydride under reduced pressure. The solvent was stored over a Type 4 Å molecular sieve (dried in an oven at 300°C overnight).¹² PhCN (Aldrich; 99.9% HPLC) was dried over magnesium sulfate, then distilled at normal pressure. MeOH, (Fission; HPLC-grade) was used without further purification.

The macrocycles **1** and **2** were synthesized at the Thermochemistry Laboratory according to the procedure reported in the literature.¹³ These were dried in a piston drier at 100°C for several days before use.

Deuterated acetonitrile, CD₃CN, deuterated methanol, CD₃OD, and deuterated DMF, C₃D₇NO, and tetramethylsilane, TMS, were purchased from Aldrich.

¹H NMR Measurements. ¹H NMR measurements were recorded at 298 K using a Bruker AC-300E pulsed Fourier transform NMR spectrometer. Typical operating conditions for routine proton measurements involved “pulse” or flip angle of 30°, spectral frequency (SF) of 300.135 MHz, delay time of 1.60 s, acquisition time (AQ) of 1.819 s, and line broadening of 0.55 Hz.

Solutions of the samples under investigation were prepared in the appropriate deuterated solvent and then placed in 5-mm NMR tube using TMS as internal reference.

The complexation behavior of the ligands (**1** and **2**) toward metal cations was studied by adding the metal-ion salt (8.0×10^{-3} – 1.6×10^{-2} mol dm⁻³) into the NMR tube containing the ligand dissolved in the appropriate solvent (8.0×10^{-4} – 1×10^{-3} mol dm⁻³). Stepwise additions of the metal-ion salt were made and chemical shifts were recorded. Changes in chemical shifts upon addition of the metal-ion salt relative to the free ligand were calculated.

Conductance Measurements. For these measurements, a Wayne-Kerr Autobalance Universal Bridge, type B642, was used.

The Wayne-Kerr meter was connected to a glass-bodied Russel platinum electrode unit. The reaction took place in a cylindrical glass vessel (with lid) wrapped in a thermostated jacket and maintained at 298.15 K with a water bath. A magnetic stirrer was used to keep homogeneous the solutions throughout the experiment.

The conductance cell constant was determined by adding in steps an aqueous solution of KCl (0.1000 mol·dm⁻³) to the deionized water in the cell.

Potassium chloride was recrystallized from deionized water and dried at 120°C for 3 days prior to use.

The conductance readings followed each injection and were recorded after allowing enough time for the solution to attain thermal equilibrium.

The conductance of the deionized water was measured in advanced and subtracted from each conductance reading. The corresponding molar conductances (Λ_m, S·cm²·mol⁻¹) were calculated from the equation of Lind, Zwolenik, and Fuoss.¹⁴ The molar conductance of the KCl (0.1000

(8) Danil de Namor, A. F.; Cleverly, R. M.; Zapata-Ormachea, M. L. *Chem. Rev.* **1998**, *98*, 2495; see also references therein.

(9) Danil de Namor, A. F. In *Calixarenes 2001*; Asfari, Z., Böhrner, V., Harrowfield, I. M., Vicens, J., Eds.; Kluwer Academic Publishers: Dordrecht, The Netherlands, 2001; Chapter 19.

(10) Danil de Namor, A. F.; Gil, E.; Llosa Tanco, M. A.; Pacheco Tanaka, D. A.; Pulcha Salazar, L. E.; Schulz, R. A.; Wang, J. *J. Phys. Chem.* **1995**, *99*, 16781.

(11) Perrin, D. D.; Armarego, W. L. F.; Perrin, D. R. *Purification of Laboratory Chemicals*, 2nd ed.; Pergamon Press Ltd.: Oxford, U.K., 1980.

(12) Furniss, B. S.; Hannaford, A. J.; Smith, P. W. G.; Tatchell, A. R.; *Textbook of Practical Organic Chemistry*, 5th ed.; Longman Group UK Limited: , 1989.

(13) Danil de Namor, A. F.; Hutcherson, R. G.; Sueros Velarde, J. F.; Alvarez-Larena, A.; Briansó, J. L. *J. Chem. Soc., Perkin Trans. 1* **1988**, 2933.

(14) Lind, J. F.; Zwolenik, J. J.; Fuoss, R. M. *J. Phys. Chem.* **1965**, *81*, 1557.

Table 1. Crystal Data and Structure Solution Methods and Refinement Results for the Cadmium and Lead Complexes with the Ethylester Calixarene

	cadmium (3)	lead (4)
empirical formula	C ₆₈ H ₉₂ CdCl ₂ N ₄ O ₂₀	C ₇₂ H ₁₀₄ Cl ₂ N ₆ O ₂₂ Pb
formula weight	1468.76	1683.70
temperature (K)	120(2)	120(2)
low-temperature device		Oxford Cryosystems
cooling rate		200 K/h
crystal system	orthorhombic	monoclinic
space group	Pbca	P2 ₁ /c
unit cell dimensions ^a		
<i>a</i> (Å)	20.4360(2)	16.7310(3)
<i>b</i> (Å)	19.6950(2)	13.7050(5)
<i>c</i> (Å)	35.1220(4)	35.4330(12)
β (°)	90.00	90.537(2)
volume(Å ³)	14136.1(3)	8124.4(4)
<i>Z</i> , calcd density (Mg/m ³)	8, 1.380	4, 1.377
absorpt.coef (μ , mm ⁻¹)	0.459	2.215
<i>F</i> (000)	6160	3480
crystal size (mm)	0.15 × 0.15 × 0.20	0.20 × 0.20 × 0.25
crystal color/shape	colorless/fragment	colorless/fragment
diffractometer/scan		kappaCCD/ φ and ω
radiat., graph. monochr.		MoK α , λ = 0.71073 Å
ϑ range for data coll.	3.22 to 25.00°	1.22 to 24.80°
index ranges	-24 ≤ <i>h</i> ≤ 24, -23 ≤ <i>k</i> ≤ 23, -41 ≤ <i>l</i> ≤ 41	-19 ≤ <i>h</i> ≤ 19, -16 ≤ <i>k</i> ≤ 16, -33 ≤ <i>l</i> ≤ 41
reflections collected	23025	28224
independent reflections	12217 [<i>R</i> (int)=0.026]	12972 [<i>R</i> (int)=0.048]
completeness	90.9% (to ϑ = 25.0°)	88.6% (to ϑ = 24.8°)
absorption correction	multiscan ¹⁶	
max and min transm.	0.572 and 0.487	
obs. reflects. [<i>I</i> > 2 σ (<i>I</i>)]	10517	10969
data collection		COLLECT ¹⁷
data reduct. and correct. ^b		DENZO and SCALEPACK ¹⁸
and struct. solut. ^c and		SHELXS-97 ¹⁹
refinement ^d programs		SHELXL-97 ¹⁹
refinement method		full-matrix least-squares on <i>F</i> ²
weights, <i>w</i>	$[\sigma^2(F_o^2) + (0.013P)^2 + 33.2P]^{-1}$	$[\sigma^2(F_o^2) + (0.02P)^2 + 173P]^{-1}$
<i>P</i> = [max(<i>F_o</i> ² , 0) + 2 <i>F_c</i> ²]/3		
12217/0/876	12972/25/950	
goodness-of-fit on <i>F</i> ²	1.120	1.176
final <i>R</i> indic.	[<i>I</i> > 2 σ (<i>I</i>)] <i>R</i> 1=0.047, <i>wR</i> 2=0.114	<i>R</i> 1=0.077, <i>wR</i> 2=0.172
<i>R</i> indices (all data)	<i>R</i> 1=0.057, <i>wR</i> 2=0.120	<i>R</i> 1=0.092, <i>wR</i> 2=0.179
larg. peak and hole(e.Å ⁻³)	0.496 and -0.613	3.43 ^f and -2.64

^a Least-squares refinement of the angular settings for 23025 reflections in the 3.22 < ϑ < 25° range for the cadmium complex and 28224 reflections in the 1.22 < ϑ < 24.80° range for the lead complex. ^b Corrections: Lorentz and polarization. Empirical absorption correction was applied to the lead complex but not to the cadmium one as μ times the largest crystal dimension was less than 0.1. ^c Neutral scattering factors and anomalous dispersion corrections. ^d Structure solved by direct and Fourier methods. The final molecular model obtained by anisotropic full-matrix least-squares refinement of the non-hydrogen atoms. ^e *R* indices defined as $R1 = \sum ||F_o| - |F_c|| / \sum |F_o|$, $wR2 = [\sum w(F_o^2 - F_c^2)^2 / \sum w(F_o^2)^2]^{1/2}$. ^f Close to a disordered perchlorate ion.

mol dm⁻³ in water at 298.15 K) was used to calculate the corresponding values of the specific conductance and then the cell constant.

For conductometric titrations, the cell was filled with the metal-ion salt solution prepared in the appropriate solvent (~25 cm⁻³), reweighed, sealed, and left under stirring during the titration to reach thermal equilibrium. Then, a solution of the ligand was added in steps using a hypodermic syringe.

To test for ion-pair formation in solution, conductance measurements were performed at different electrolyte concentration as described elsewhere.¹⁵

X-ray Diffraction Data. Crystal data, data collection procedure, structure determination methods, and refinement results for the cadmium and lead complexes with the ethylester derivative (complexes **3** and **4** respectively) are summarized in Table 1.^{16–19} The corresponding data for the metal complexes with the methyl ketone derivative (**5** and **6**) are listed in Table 2.

(15) Onsager, L. *Physik. Z.* **1927**, *28*, 277.

(16) Blessing, R. H. *Acta Cryst.* **1995**, *A51*, 33.

(17) Enraf-Nonius (1997–2000) Collect. Nonius, B. V., Delft, The Netherlands.

(18) Otwinowski, Z.; Minor, W. In *Methods in Enzymology*; Carter, C. W., Jr., Sweet, R. M., Eds.; Academic Press: New York, 1997; p 307.

(19) Sheldrick, G. M. *SHELXL-97. Program for Crystal Structure Analysis*; University of Gottingen: Gottingen, Germany, 1997.

Complex 3. The hydrogen atoms of the calixarene ligand and the MeCN solvent it hosts were found in a different Fourier map along with a few H-atoms of the crystallization acetonitrile molecules. However, all the hydrogen atoms were positioned stereochemically and refined with the riding method. The methyl H-atoms were treated in the refinement as rigid bodies and allowed to rotate around the corresponding C–C bond such as to maximize the sum of the observed electron density at the three calculated H-positions.

Complex 4. The samples turned out to diffract poorly. One of the perchlorate anions showed large rotational disorder, and therefore it was refined with Cl–O and O···O distances restrained to target values of 1.43 (1) and 2.35(1) Å, respectively. A difference Fourier map phased on the lead and acetonitrile complex and the perchlorate ions showed a residual electron density that could be interpreted in terms of two water molecules and five disordered acetonitrile molecules. The latter molecules were refined with C–N and C–C distances restrained to target values of 1.15 (1) and 1.43 (1) Å, respectively. A further difference Fourier map showed about half of the hydrogen atoms. However, all H-atoms, except the water hydrogens, were positioned and refined as described for complex **3**.

Complex 5. The hydrogen atoms of the calixarene ligand and the MeCN solvent it hosts were found in a difference Fourier map along

Table 2. Crystal Data and Structure Solution Methods and Refinement Results for the Cadmium and Lead Complexes with the Methyl Ketone Calixarene

	cadmium (5)	lead (6)
empirical formula	C ₆₈ H ₉₀ CdCl ₂ N ₆ O ₁₆	C ₆₂ H ₈₁ Cl ₂ N ₃ O ₁₆ Pb
formula weight	1430.76	1402.39
temperature (K)	120(2)	100(2)
low-temperature device		Oxford Cryosystems
cooling rate		200 K/h
crystal system	triclinic	orthorhombic
space group	P-1 (No. 2)	<i>Fdd2</i> (No. 43)
unit cell dimensions ^a		
<i>a</i> (Å)	13.5880(1)	36.5770(1)
<i>b</i> (Å)	16.7700(2)	57.4930(2)
<i>c</i> (Å)	16.7780(2)	12.2800(4)
α (°)	82.683(1)	90.00
β (°)	79.878(1)	90.00
γ (°)	66.743(1)	90.00
volume(Å ³)	3450.77(6)	25823.9(8)
Z, calc. density (Mg/m ³)	2, 1.377	16, 1.443
absorpt. coeff.(μ ,mm ⁻¹)	0.464	2.763
<i>F</i> (000)	1500	11488
crystal size(mm)	0.36 × 0.30 × 0.24	0.44 × 0.22 × 0.20
crystal color/shape		colorless/fragment
diffractometer/scan		kappaCCD/ ϕ and ω
radiat., graph. monochr.		MoK α , λ =0.71073 Å
θ range(°)data collect.	2.26 to 27.50	2.83 to 25.00
index ranges	-17 ≤ <i>h</i> ≤ 17, -21 ≤ <i>k</i> ≤ 21, -21 ≤ <i>l</i> ≤ 21	0 ≤ <i>h</i> ≤ 43, 0 ≤ <i>k</i> ≤ 68, -14 ≤ <i>l</i> ≤ 14
reflections collected	56483	15921
independent reflections	15757 [R(int)=0.063]	11144 [R(int)=0.029]
completeness	99.4% (to θ = 27.5°)	99.6% (to θ = 27.0°)
absorption correction	Multiscan ¹⁶	
max and min transm.	0.897 and 0.851	0.608 and 0.376
obs. reflects.[I > 2 σ (I)]	14309	10909
data collection		COLLECT ¹⁷
data reduct. and correct. ^b		DENZO and SCALEPACK ¹⁸
and struct. solut. ^c and		SHELXS-97 ¹⁹
refinement ^d programs		SHELXL-97 ¹⁹
refinement method		full-matrix least-squares on <i>F</i> ²
weights, <i>w</i>	$[\sigma^2(F_o^2) + (0.045P)^2 + 2.6P]^{-1}$	$[\sigma^2(F_o^2) + (0.062P)^2 + 296P]^{-1}$
$P = [\max(F_o^2, 0) + 2F_c^2]/3$		
data/restraints/param.	15757/0/850	11144/4/767
goodness-of-fit on <i>F</i> ²	1.05	1.08
final <i>R</i> indic.[I > 2 σ (I)] ^e	<i>R</i> 1=0.0361, <i>wR</i> 2=0.0919	<i>R</i> 1=0.0335, <i>wR</i> 2=0.0991
<i>R</i> indices (all data)	<i>R</i> 1=0.0408, <i>wR</i> 2=0.0966	<i>R</i> 1=0.0344, <i>wR</i> 2=0.1000
larg. peak and hole(e.Å ⁻³)	0.806 and -1.373	0.898 and -1.036

^a Least-squares refinement of the angular settings for 56483 reflections in the 2.26 < θ < 27.50° range for the cadmium complex and 14460 reflections in the 0.998 < θ < 27.485° range for the lead complex. ^b Corrections: Lorentz, polarization, and empirical absorption correction. ^c Neutral scattering factors and anomalous dispersion corrections. ^d Structure solved by direct and Fourier methods. The final molecular model obtained by anisotropic full-matrix least-squares refinement of the non-hydrogen atoms. ^e *R* indices defined as: *R*1 = $\sum ||F_o| - |F_c|| / \sum |F_o|$, *wR*2 = $[\sum w(F_o^2 - F_c^2)^2 / \sum w(F_o^2)^2]^{1/2}$.

with a few H-atoms from the crystallization acetonitrile molecules. However, all the hydrogen atoms were positioned and refined as described above.

Complex 6. About half of the H-atoms were found among the first one hundred peaks of a difference Fourier map. Also here, the hydrogen atoms were treated in a refinement as described for the other complexes.

Calorimetric Titrations. For macrocalorimetric titrations (direct and competitive), the Tonac 450 calorimeter was used as an isoperibol titration calorimeter.²⁰ It is equipped with a 2 cm³ buret connected by a silicone tube to the reaction vessel. The reproducibility of the apparatus was checked carrying out the standard reaction of protonation of an aqueous solution of tris(hydroxymethyl)aminomethane (THAM) in hydrochloric acid (HCl, 0.1 mol dm⁻³) at 298.15 K.²¹ The value determined -47.44 ± 0.11 kJ·mol⁻¹ is in agreement with the one reported by Hill, Öjelund, and Wadsö²² using an LKB reaction calorimeter.

For stability constant values lower than 10⁶, (log *K*_s = 6), direct calorimetric titrations were performed. A solution of perchlorate salt of selected metal ions (2.0–5.0 × 10⁻² mol dm⁻³) was prepared in acetonitrile, placed in the buret, and titrated into the vessel containing a solution of the free ligand (**1** or **2**), (50 cm³, 6.0 × 10⁻⁴–1.5 × 10⁻³ mol dm⁻³) prepared in the same solvent.

For log *K*_s values higher than 6, competitive calorimetric titrations were performed. A solution of the metal-ion salt (2.0–5.0 × 10⁻² mol dm⁻³) was prepared in acetonitrile, placed in the buret, and titrated into the vessel containing a solution of the ligand (**1** or **2**) complexed with a metal cation (Mⁿ⁺), (50 cm³, **1** or **2**, 6.0 × 10⁻⁴ to 1.5 × 10⁻³ mol dm⁻³; *n*_{Mn+} = 3 *n*_{1 or 2}; where *n*_{Mn+} and *n*_{1 or 2} are the number of moles of the metal cation in the vessel and the ligand **1** or **2**, respectively), prepared in the same solvent. The stability constant of the complex in the vessel was lower than that expected between the ligand (**1** or **2**) and the metal cation under investigation placed in the buret, enabling the latter to compete and replace the metal cation of the complex in the vessel.

The whole system was then immersed in a thermostated water bath at 298.15 K and allowed to reach thermal equilibrium.

Furthermore, the titration was carried out in recorded time intervals. A chart recorder was used to monitor the reaction taking place in the

(20) Christensen, J. J.; Izatt, R. M.; Hansen, L. D. *Rev. Sci. Instrum.* **1965**, *36*, 779.

(21) Eatough, D. J.; Christensen, J. J.; Izatt, R. M. *Experiments in Thermometric Titrimetry and Titration Calorimetry*; Brigham Young University Press: Provo, UT.

(22) Hill, J. O.; Öjelund, G.; Wadsö, I. *J. Chem. Thermodyn.* **1969**, *1*, 111.

vessel. Corrections for the heat of dilution were also made by titrating the solution in the buret into the vessel with the solvent of interest. An electrical calibration was carried out after each titration experiment.

Thermodynamic parameters for a single system were determined at different concentrations of the metal-ion salt, to ensure that no ion-pair formation occurred within the working concentration range. All measurements were conducted in triplicate.

For microcalorimetric titrations (direct and competitive), the four-channel heat conduction microcalorimeter (Thermometric 2277) designed by Suurkuusk and Wadsö²³ was used. Electrical (static and dynamic) and chemical calibrations were carried out to check the reliability of the equipment.²⁴

The reaction vessel was charged with 2.8 cm³ of the ligand (6.0×10^{-4} to 1.5×10^{-3} mol dm⁻³) in the appropriate solvent. The metal-ion salt (1.4×10^{-2} to 3.5×10^{-2} mol dm⁻³) was injected incrementally using a 0.5 cm³ gastight motor driven Hamilton syringe. In each titration experiment, about 20 injections were made at time intervals of 30–45 min. Corrections for the enthalpy of dilution of the titrant in the solvent were carried out in all cases. A computer programme for TAM (Digitam 4.1 for Windows from Thermometric AB and Scitech Software AB, Sweden) was used to calculate the log K_s and $\Delta_c H^\circ$ values for the process under study.

The same procedure and methodology for the competitive titration were used for micro and macro calorimetric measurements.

Preparation of the Lead(II) and Cadmium(II) Complexes of 1 and 2 with Acetonitrile. Stoichiometric quantities of the metal-ion perchlorate salt and the appropriate ligand dissolved in acetonitrile were mixed. These were left for several days at room temperature until crystals were formed. The crystals were isolated, and microanalysis was carried out at the University of Surrey. Lead(II) complex of **1** requires % C, 51.68; H, 5.56; N, 0.97; found, % C, 51.70; H, 5.81; N, 0.97; while the lead(II) complex of **2** requires % C, 52.76; H, 5.68; N, 1.06; found, % C, 52.35; H, 5.73; N, 1.05. The cadmium(II) complex of **1** requires % C 55.36; H, 6.18; N, 1.04; found % C, 55.34; H, 6.22; N, 1.02; while the cadmium(II) complex of **2** requires % C, 56.84; H, 6.12; N, 1.14; found % C, 56.79; H, 6.17; N, 1.15.

Results and Discussion

¹H NMR Studies. ¹H NMR measurements involving **1** and **2** and bivalent cations, Mg²⁺, Ca²⁺, Sr²⁺, Ba²⁺, Pb²⁺, Zn²⁺, Cd²⁺, Hg²⁺, Co²⁺, Ni²⁺ as perchlorates, were carried out in various solvents, CD₃CN, CD₃OD, and C₃D₇NO at 298 K. Chemical shift changes upon the addition of the appropriate salt of selected metal ions to the appropriate ligand (**1** or **2**) were only observed for alkaline-earth and heavy-metal cations in CD₃CN and these are shown in Table 3. Indeed, the addition of bivalent cations to the ligand in CD₃OD and C₃D₇NO did not lead to changes in the chemical shifts of the ligand. A quick inspection of the ¹H NMR spectra of **1** and **2** (see footnote Table 3) shows the characteristic pair of doublets of the bridging methylene protons (ArCH₂Ar) which appear in the spectrum when the calix(4)arene is in the cone conformation in solution.

Gutsche²⁵ has noted that the difference in the chemical shifts ($\Delta\delta$ ppm) between the axial and equatorial protons serves as a measure of the flattening of the cone. The values of **1** and **2** are 1.55 and 1.56 ppm, respectively. The fact that these values are greater than 0.90 ppm indicate that the aromatic rings in **1** and **2** become more parallel to each other while the macrocycle adopts a distorted cone conformation. Data in Table 3 show that upon complexation with these cations in CD₃CN, the axial protons

Table 3. Chemical Shift Changes ($\Delta\delta$ ppm)^a in the ¹H NMR Spectra of **1** and **2** with Bivalent Cations in CD₃CN at 298 K

	H-1	H-2	H-3 (equatorial)	H-3 (axial)	H-4	H-5	H-6
Mg ²⁺	0.07	0.48	0.39	overlap	0.16	0.24	0.15
Ca ²⁺	0.07	0.48	0.44	-0.77	0.01	0.29	0.16
Sr ²⁺	0.07	0.48	0.39	-0.69	-0.03	0.30	0.15
Ba ²⁺	0.10	0.45	0.36	-0.55	-0.22	0.27	0.12
Pb ²⁺	0.10	0.49	0.43	-0.56	0.04	0.29	0.16
Cd ²⁺	0.08	0.49	0.43	-0.65	-0.02	0.29	0.15
Hg ²⁺	0.07	0.47	0.45	-0.72	-0.01	0.30	0.15

	H-1	H-2	H-3 (equatorial)	H-3 (axial)	H-4	H-5
Mg ²⁺	0.02	0.33	0.35	-0.75	0.32	0.17
Ca ²⁺	0.02	0.32	0.32	-1.02	0.17	0.21
Sr ²⁺	0.02	0.33	0.33	-0.90	0.09	0.14
Ba ²⁺	0.06	0.30	0.23	-0.76	-0.05	0.05
Pb ²⁺	0.06	0.34	0.29	-0.68	0.23	0.16
Cd ²⁺	0.02	0.33	0.34	-0.40	0.14	0.21
Hg ²⁺	0.03	0.33	0.36	-0.94	0.14	0.25

^a Relative to the free ligand. Chemical shifts for **1**, (ppm); H-1 = 1.12; H-2 = 7.02; H-3(eq.) = 3.26; H-3(ax.) = 4.81; H-4 = 4.769; H-5 = 4.17; H-6 = 1.27 ppm. Chemical shifts for **2**, (ppm); H-1 = 1.16; H-2 = 7.14; H-3(eq.) = 3.28; H-3(ax.) = 4.84; H-4 = 4.11; H-5 = 2.18 ppm.

are deshielded while the equatorial protons are shielded. As a result, shift differences between the pair of doublets decrease from the free to the complex ligands.

These changes imply that the aromatic rings of the hydrophobic cavity are now adopting a flatter, more parent conelike conformation as the pendant arms of the ligand are moving closer together to coordinate to the metal cation. Chemical shift changes are more pronounced for Ca(II) relative to the other metal cations.

Significant chemical shift changes observed in Table 3 are those for the aromatic protons (H-2). These are more significant for the ester than for the ketone derivatives, suggesting that the change in conformation in the hydrophobic cavity upon complexation is similar for all cations.

For both ligands, the variation of the chemical shifts of H-4 is linearly correlated with the cation size with the exception of Pb(II) and Cd(II) as shown in Figure 2. However, the deshielding effect upon complexation is more pronounced for the ketone (higher dipole moment; $\mu = 2.8$ D) than for the ester derivative ($\mu = 1.72$ D).²⁶

The chemical shift changes observed for H-5 in both ligands are more significant for the ester relative to the ketone functionalized calix(4) arene. While the cation effect on H-5 is quite significant in **2**, only small variations are observed for **1**. These findings may be attributed to the less bulky methyl group in **2** relative to **1**. To assess the composition of the metal-ion complexes, conductometric titrations were carried out and these are now discussed.

Conductometric Titrations. The main aim of conductance measurements was to establish the composition of the metal-ion complexes in acetonitrile, information that is required to proceed with the thermodynamic characterization of the complexation process involving these systems in this solvent.

Plots of molar conductance (Λ_m) against the ligand/metal ion mole ratio showed either well-defined changes of curvature (moderate complexation, Ba²⁺, Cd²⁺, and Hg²⁺) or two straight

(23) Suurkuusk, J.; Wadsö, I. *Scr.-Chim.* **1982**, *20*, 155.

(24) LKB 2277 *Thermal Activity Monitor, Instruction Manual*; LKB Produkter AB: Bromma, Sweden, 1985.

(25) Gutsche, C. D. *Aldrichimica Acta* **1995**, *28*, 3.

(26) McMurry, J. *Organic Chemistry*, 5th ed.; Brooks/Cole: Pacific Grove, CA, 2000.

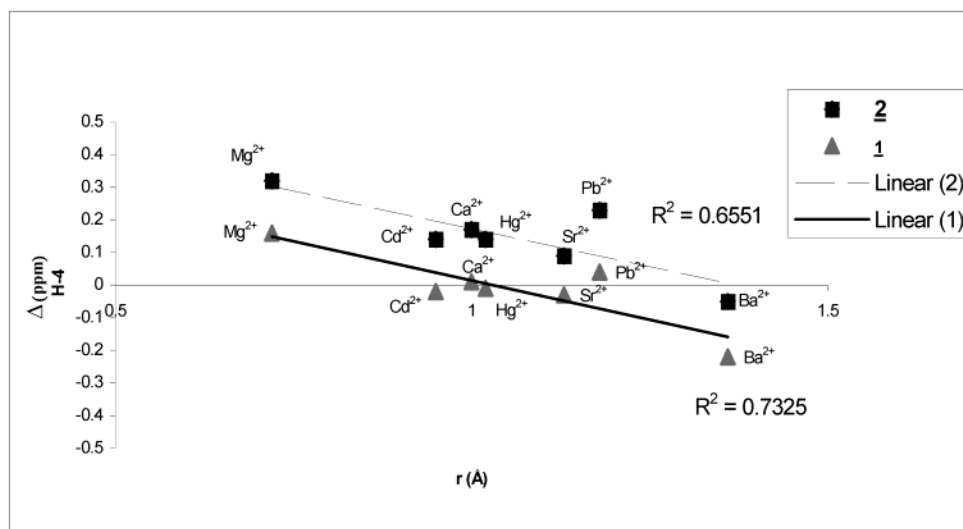


Figure 2. Chemical shift changes (ppm) of H-4 for ligands **1** and **2** vs cation size.

lines intersecting (strong complexation, Ca^{2+} , Sr^{2+} , Pb^{2+}) at the 1:1 mole ratio indicating that one metal cation interacts per unit of **1** or **2**.

Representative examples are shown in Figure 3 for the Ba^{2+} -**2** and the Pb^{2+} -**1** systems in acetonitrile at 298.15 K.

The conductometric titration curves, (Figure 3), show a decrease in the molar conductance upon the addition of the ligand into the solution containing the metal cations in acetonitrile. This implies that as the size of the cation increases in going from the free to the complex cation, the mobility decreases.

Plots with slight (or nonexistent) slope and without any indication of a change in slope at any given mole ratio were found for Zn^{2+} , Ni^{2+} , Co^{2+} , and these ligands in acetonitrile. These findings are in agreement with ^1H NMR measurements where no chemical shift changes were observed by the addition of the latter three cations to the ligands in CD_3CN . These results suggest that very weak or no complexation occurs between these ligands and these cations in acetonitrile.

As far as bivalent metal cations are concerned, in an attempt to assess the medium effect on the complexation process, we proceeded with conductometric titrations in *N,N*-dimethylformamide, methanol, and benzonitrile at 298.15 K. The curves recorded did not show any break point at any stoichiometry suggesting that no complexation takes place between these cations and these ligands in these solvents. These findings lead us to investigate further the role of acetonitrile in the binding of bivalent cations and these ligands. Therefore, on the basis of the conductance results obtained for Pb^{2+} and Cd^{2+} with these ligands, we proceeded with the isolation of the metal-cation complexes and their X-ray characterization as described in the following section.

X-ray Diffraction Studies on Lead and Cadmium Complexes of 1 and 2. Fractional coordinates and equivalent isotropic displacement parameters for the cadmium and lead complexes of **1** and **2** (perchlorate as counterion) and intramolecular bond distances and angles are available as Supporting Information. The corresponding ORTEP drawings of complexes **3–6** are shown in Figures 4–7, respectively.

In all four compounds, the macrocycle hosts a metal cation ($\text{M}^{2+} = \text{Cd}^{2+}$ and Pb^{2+}) within the hydrophilic pocket while

the hydrophobic cavity is filled with an acetonitrile solvent molecule. An interesting feature of these compounds is found in the cadmium complexes, **3** and **5** which in contrast to most other calix[4]arene complexes, the solvent molecule is found with the CN end pointing inward to form a Cd–N bond. The orientation of acetonitrile in **3** and **5** is opposite to that found in **4** and **6**, the free ligand **2**, and in most of the X-ray structures reported in the literature.^{27–31} This fact strongly suggests that depending on the nature of the cation, interaction in the hydrophilic cavity preorganizes the hydrophobic cavity as to host a molecule of acetonitrile oriented in such a way as to optimize its binding in the complex (allosteric effect). As shown in Figures 4 and 6, for **3** and **5** respectively, the coordination number of the cation is altered from 9 (**3**) to 8 (**5**). For **3**, the 9-fold coordination is achieved through the four ethereal oxygen atoms [Cd–O distances in the range from 2.378 (2) to 2.412 (2) Å], the four carbonyl oxygen atoms [d (Cd–O) distances from 2.382 (2) to 2.610 (2) Å], and the nitrogen atom of the acetonitrile molecule hosts by the calix [Cd–N distance; 2.465 (3) Å].

Thus, the ligand atoms conform the corners of a capped archimedean antiprism with the N– atom at the capping site. The ethereal and carbonyl oxygen atoms lay on the two distinct squares bases, which are about 2.24 Å apart and tilted 37° from each other. The Cd(II) cation is sandwiched between these two bases and is closer to the ethereal oxygens plane (0.688 (1) Å) than to the carbonyl oxygens (1.553 (1) Å).

As far as **5** is concerned, the 8-fold coordination achieved by this compound is striking, given that besides the four ethereal oxygen atoms [Cd–O distances from 2.374 (1) to 2.417 (1) Å], three (instead four as in **3**) of the four carbonyl oxygen

(27) Abdi, R.; Baker, M. V.; Harrowfield, J. M.; Ho, D. S.-C.; Richmond, W. R.; Skelton, B. W.; White, A. H.; Varnek, A.; Wipff, G. *Inorg. Chim. Acta* **1996**, *246*, 275.

(28) Varnek, A.; Sirlin, C.; Wipff, G. *Crystallography of Supramolecular Compounds*; International School of Crystallography, NATO ASI, Kluwer Academic: Dordrecht, The Netherlands, 1996; p 67.

(29) Danil de Namor, A. F.; Piro, O. E.; Pulcha Salazar, L. E.; Aguilar-Cornejo, A. F.; Al-Rawi, N.; Castellano, E. E.; Sueros Velarde, F. J. *J. Chem. Soc., Faraday Trans.* **1998**, *94*, 3097.

(30) Danil de Namor, A. F.; Castellano, E. E.; Pulcha Salazar, L. E.; Piro, O. E.; Jafou, O. *Phys. Chem. Chem. Phys.* **1999**, *1*, 285.

(31) Danil de Namor, A. F.; Kowalska, D.; Castellano, E. E.; Piro, O. E.; Sueros Velarde, F. J.; Villanueva-Salas, J. *Phys. Chem. Chem. Phys.* **2001**, *3*, 4010.

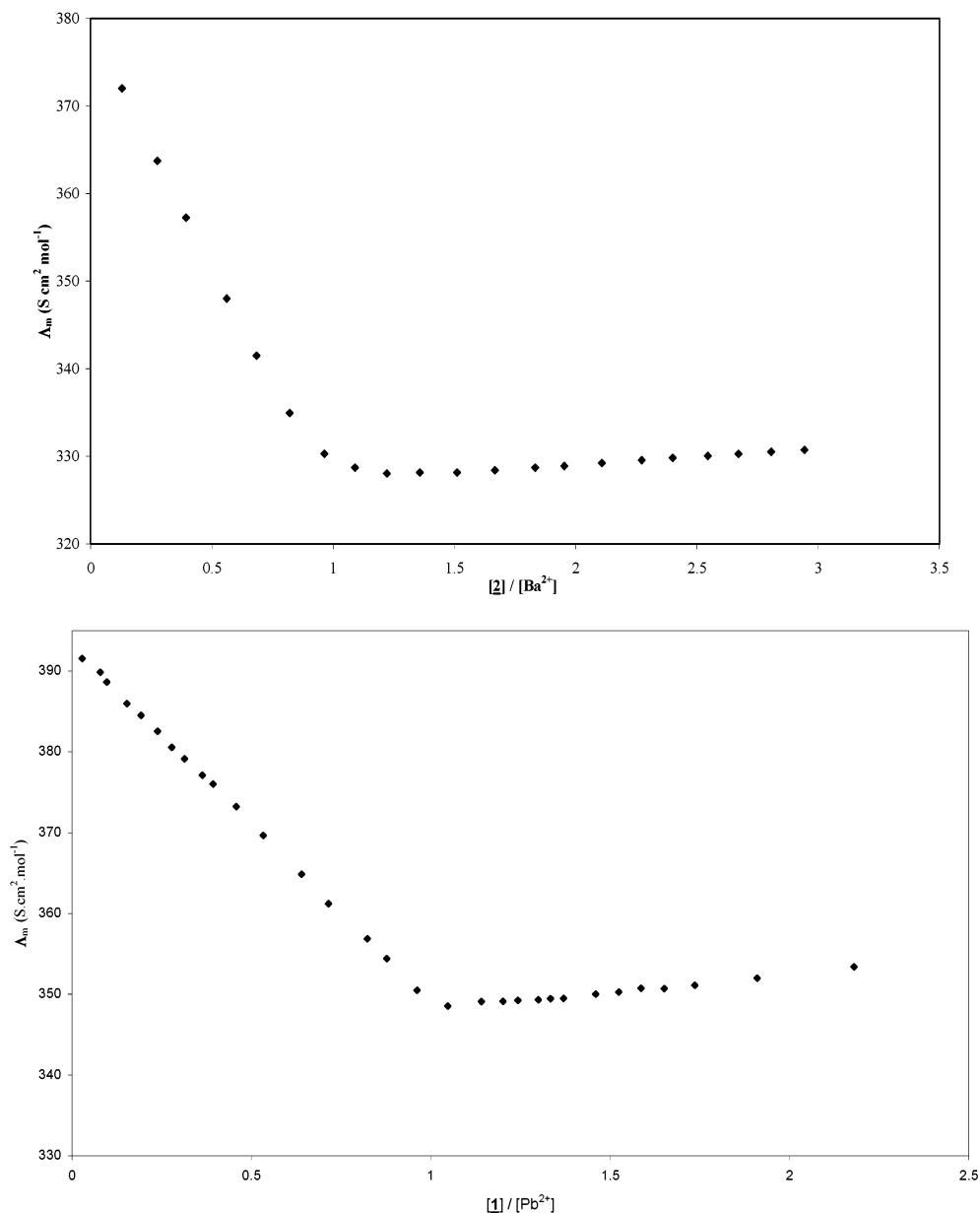


Figure 3. Conductometric titration curves for Ba^{2+} -**2** and Pb^{2+} -**1** systems in acetonitrile at 298.15 K.

atoms of **5** [d (Cd–O) distances from 2.370 (1) to 2.377 (1) Å] interact with the cation. The eight coordination site is provided by the nitrogen atom of the acetonitrile solvent molecule [Cd–N distance; 2.428 (2) Å]. The remarkable change in the polyhedral environment around cadmium in **5** relative to **3** may be attributed to the fact that the less bulky terminal group of the methyl ketone pendant arm relative to that of the ethyl ester derivative allows a more compact and closer arrangement of the coordinated carbonyl oxygen atoms to cadmium (in about 0.12 Å) in terms of three rather than the four oxygen atoms found in the ethyl ester complex **3**. Alternatively, we may attribute the change of coordination around Cd(II) in **5** relative to **3** as promoted by the relatively less hindered pendant arm of **5** as compared with **3** which preorganize the system in a way in which a soft metal cation such as cadmium is able to select the softer binding site (nitrogen) offered by the solvent rather than the remaining hard atom (oxygen) of the ligand. This is a unique example in the field of solid-state calixarene chemistry.

The observed configuration in **5** can be described either as a distorted triangular dodecahedron or as a distorted bicapped trigonal prism. However, the rather large degree of distortion and the fact that the symmetry axes of the ideal octahedron are not even nearly parallel to the approximate symmetry axis of the calix make these descriptions of little use. We prefer then to describe the observed configuration as an irregular polyhedron defined by a top acetonitrile –N– capped square arrangement of the four ethereal oxygen atoms, nearly parallel to a triangular basis formed by three of the four carbonyl oxygen atoms [dihedral angle = 4.60 (1)°]. The square and triangular arrangements are nearly perpendicular to the metal to capping–nitrogen direction [–0.7° and 3.9° with the respective plane normal directions]. In **5**, the carbonyl oxygens point away from the coordination polyhedron as shown in Figure 6.

The environments around the metal cation in the lead complexes **4** and **6** (Figures 5 and 7) closely resemble each other, as expected from identical bite span by both the ethylester

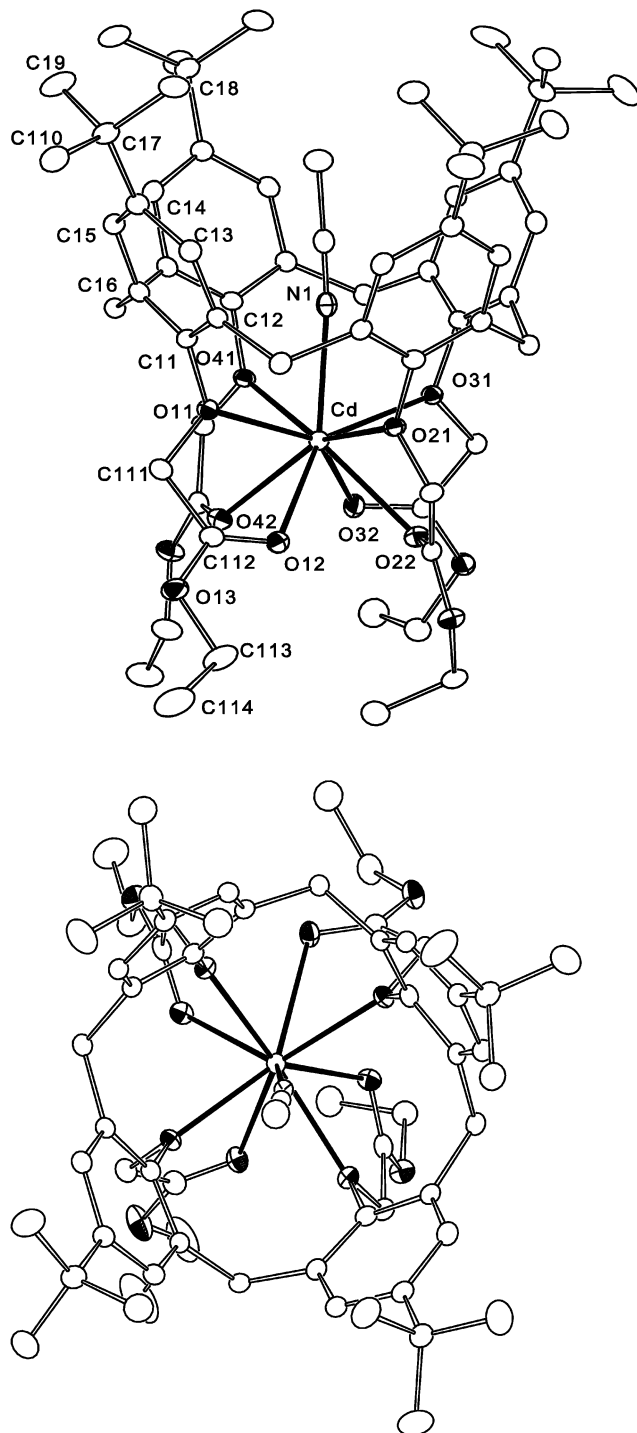


Figure 4. Side (upper) and top views of the cadmium complex with tetraethylester *p*-*tert*-butyl calix[4]arene showing the atomic displacement ellipsoids at the 30% probability level. For clarity, only one monomer has been completely labeled to show the numbering scheme. Crossed and hatched ellipsoids denote nitrogen and oxygen atoms, respectively. Cadmium-ligand bonds are indicated by full lines.

and methyl ketone pendant arms groups. The Pb(II) ion is in an 8-fold coordination with the four etheral oxygen atoms ($d(\text{Pb}-\text{O})$ distances in the range from 2.658 (6) to 2.699 (6) Å in **4** and from 2.650 (4) to 2.711 (4) Å in **6**) and the four carbonyl oxygen atoms ($d(\text{Pb}-\text{O})$ distances from 2.491 (6) to 2.527 (7) Å in **4** and from 2.492 (4) to 2.579 Å in **6**), conforming the corners of a distorted cube, tetragonally compressed along the calixarene axis. The phenol and carbonyl oxygen atoms lay on

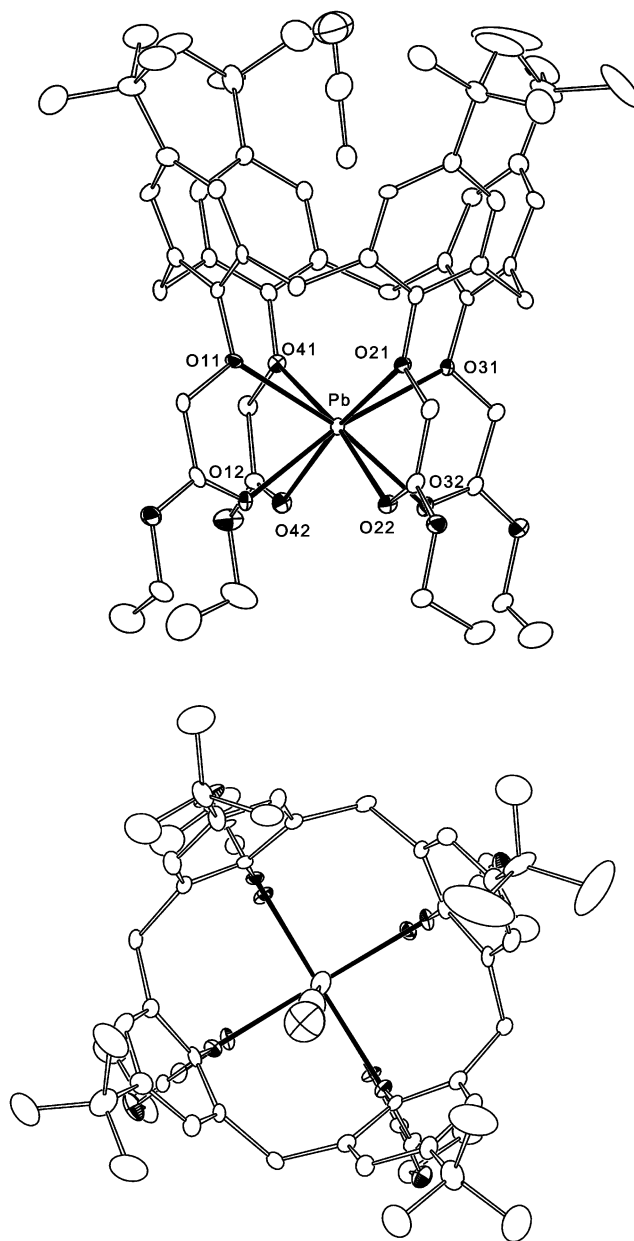


Figure 5. Side and top views of the lead complex with the tetraethylester *p*-*tert*-butyl calix[4]arene.

the two distinct square bases, which are about 2.68 Å apart and tilted in less than 2.5° from each other in both lead complexes. The Pb(II) ion is sandwiched between two bases and closer to the etheral oxygen plane (1.201 (3) Å in **4** and 1.220 (2) Å in **6**) than to the carbonyl oxygen plane (1.479 (3) Å in **4** and 1.457 (2) Å in **6**). The coordination around the Pb(II) ion in **4** and **6** in turn can be compared with the one reported for the lead complex of a tetramide calix(4)arene derivative.³² In this last complex, the metal ion is in a similar 8-fold environment with the oxygen atoms [mean Pb–O (etheral) and Pb–O (carbonyl) bond distances of 2.58 and 2.57 Å, respectively] conforming a coordination geometry intermediate between a squashed cube and an Arquimedean square antiprism. The etheral and carbonyl oxygen atoms lay at the corners of the square bases, which are 2.36 Å apart and tilted in about 27°

(32) Beer, P. D.; Drew, M. G.; Lesson, P. B.; Ogden, M. I. *J. Chem. Soc., Dalton Trans.* **1995**, 1273.

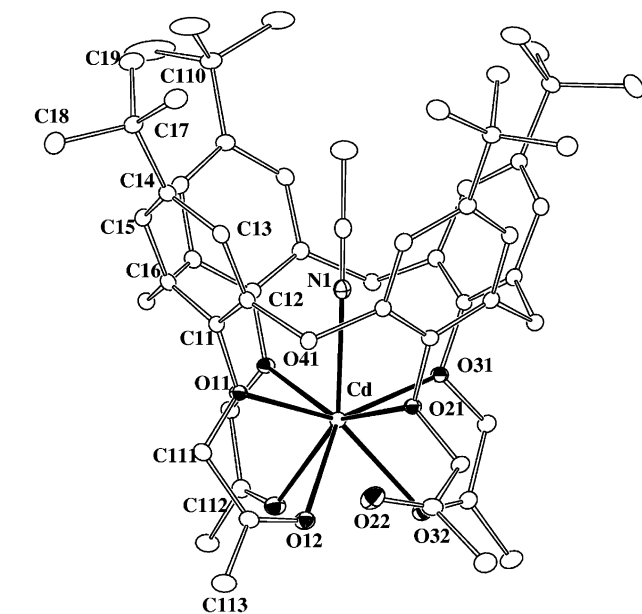


Figure 6. Side and top views of the cadmium complex with the tetramethyl ketone *p*-*tert*-butyl calix[4]arene.

from each other. As in complexes **4** and **6**, the lead cation is closer to the ethereal oxygen plane (1.14 Å) than to the carbonyl plane (1.22 Å).

As a consequence of the ionic interaction in the lower rim, all calixes (defined by the four-phenyl rings) exhibit a wide-open cone conformation. This can be described by the dihedral angles (τ) that the phenol rings subtend with the plane through the four CH₂ groups linking them. For the sake of comparison, the τ -values for all four complexes are quoted in Table 4 (obtuse τ -values indicate phenyl rings tilted so that their *tert*-butyl groups are directed away from the calix). This table also includes the interplanar angles, $\angle(\text{ph}_1, \text{ph}_3)$ and $\angle(\text{ph}_2, \text{ph}_4)$, between pair of opposite phenyl rings (see Figures 4–7) and the corresponding O11...O31 and O21...O41 cross-distances between the phenol oxygen atoms of the pendant arms.

In all compounds, the two perchlorates ions and the space-filling solvent molecules are in the periphery of the complexes at interstitial lattice sites.

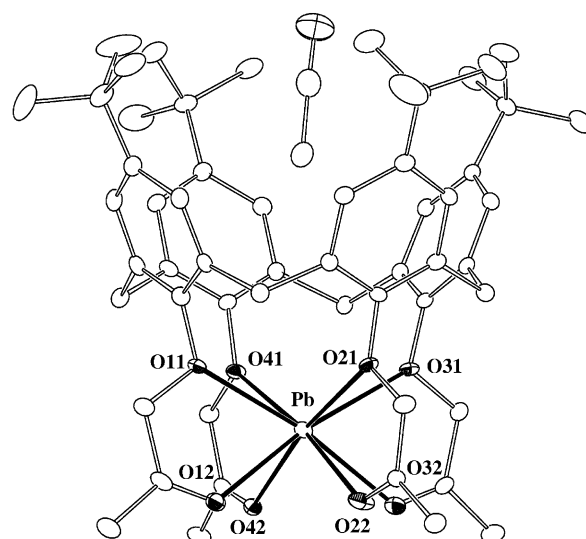


Figure 7. Side and top views of the lead complex with the tetramethyl ketone *p*-*tert*-butyl calix[4]arene.

Table 4. Dihedral Angles within the Calix and Ethernal Oxygen–Oxygen Cross-Distances of the Cd(II) and Pb(II) Complexes with the Tetraethylester and the Tetramethyl Calix[4]arene Derivatives

	cadmium (3)	lead (4)	cadmium (5)	lead (6)
$\tau_1(^{\circ})$	115.84(8)	115.3(3)	115.86(4)	113.9(1)
$\tau_2(^{\circ})$	111.29(9)	114.1(3)	111.76(4)	113.9(1)
$\tau_3(^{\circ})$	109.14(8)	112.1(3)	114.51(4)	114.7(1)
$\tau_4(^{\circ})$	116.86(8)	110.2(3)	110.82(4)	111.1(1)
$\angle(\text{ph}_1, \text{ph}_3)^{\circ}$	45.02(7)	47.6(3)	50.39(6)	48.6(2)
$\angle(\text{ph}_2, \text{ph}_4)^{\circ}$	48.17(8)	44.3(4)	42.60(6)	45.0(2)
$d(\text{O}11 \dots \text{O}31)(\text{\AA})$	4.609(3)	4.801(9)	4.565(2)	4.783(6)
$d(\text{O}21 \dots \text{O}41)(\text{\AA})$	4.561(3)	4.790(9)	4.623(2)	4.753(6)

A quantitative assessment of the selective behavior of these ligands for the metal cations is made through the thermodynamics of the complexation process, and this is discussed in the following section.

Thermodynamics of Complexation. The design of hosts with the ability of recognizing selectively one species relative

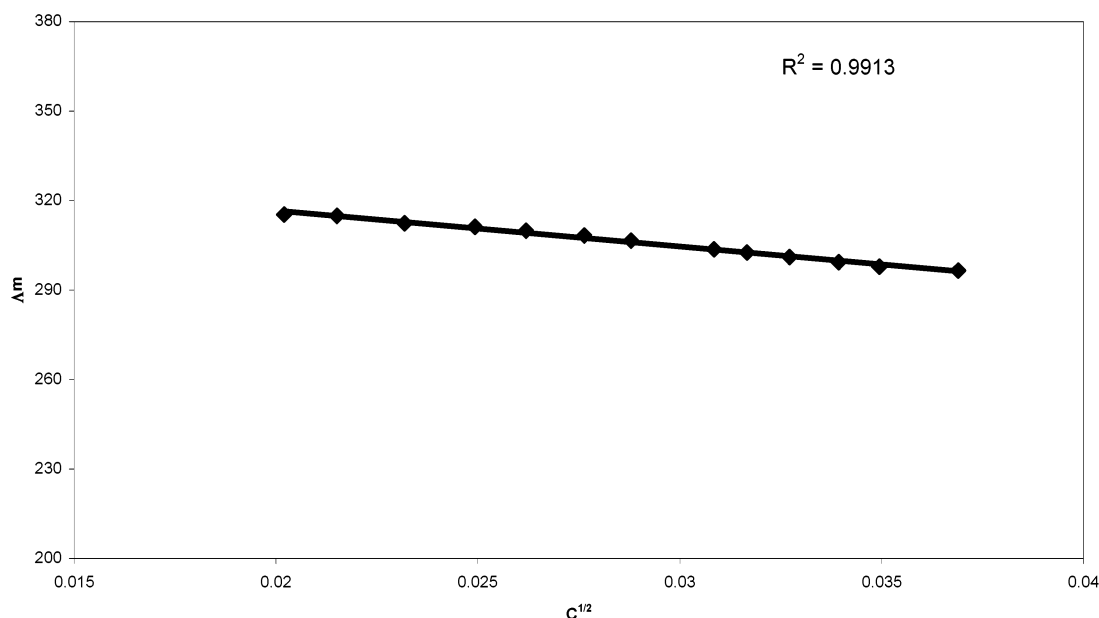


Figure 8. Molar conductance (Λ_m in $\Omega^{-1} \text{ cm}^2 \text{ mol}^{-1}$) against square root for concentration $c^{1/2}$ for $\text{Hg}(\text{ClO}_4)_2$ in acetonitrile at 298.15 K.

to another is one of the main goals of Supramolecular Chemistry. Within this context, experimental thermodynamics offers a powerful tool for the quantitative evaluation of the receptor affinity for a given cation with respect to another. There is hardly any information on the thermodynamics of complexation of calixarene derivatives and bivalent cations in the general area of calixarene chemistry.^{8,9} This is not surprising given the ancillary information required for the derivation of thermodynamics parameters for these systems. Indeed, key aspects that need to be considered in these calculations are (i) the stoichiometry of the process and (ii) the speciations present in solution particularly when multicharged cations are involved in non-aqueous media. These have a higher tendency to undergo ion-pair formation with the counterion than univalent cations.

For these purposes, conductance measurements were performed. Thus, conductometric titrations (see above) showed that both ligands (**1** and **2**) interact with these cations in acetonitrile to form 1:1 complexes.

As far as the speciations in solution are concerned, the concentrations at which the free and complex salts behave as strong electrolytes (ions in solution) in acetonitrile were established by measuring their conductance at various concentrations. An illustrative example is given in Figure 8 where a linear relationship is obtained when the molar conductance (Λ_m in $\Omega^{-1} \text{ cm}^2 \text{ mol}^{-1}$) of $\text{Hg}(\text{ClO}_4)_2$ in acetonitrile is plotted against the square root of the electrolyte concentration ($c^{1/2}$). This clearly indicates that ions are the predominant species in solution. These findings were also corroborated by performing thermodynamic studies at different electrolyte concentration, where no variations in the stability constant and enthalpy values were observed.

On the basis of the above discussion, the stability constants (expressed as $\log K_s$), standard Gibbs energies, $\Delta_c G^\circ$, enthalpies, $\Delta_c H^\circ$, and entropies, $\Delta_c S^\circ$, of complexation for bivalent cations and **1** and **2** in acetonitrile at 298.15 K listed in Table 5 are referred to the process described in eq 1.



The standard derivation of the data is also included in Table 5.

Table 5. Stability Constant ($\log K_s$) and Derived Standard Gibbs Energies, Enthalpies, and Entropies of **1** and **2** with Bivalent Cations in Acetonitrile at 298.15 K

	1	$\log K_s$	$\Delta_c G^\circ/\text{kJ}\cdot\text{mol}^{-1}$	$\Delta_c H^\circ/\text{kJ}\cdot\text{mol}^{-1}$	$\Delta_c S^\circ/\text{J}\cdot\text{K}^{-1}\cdot\text{mol}^{-1}$
Ca^{2+}		8.15 ± 0.05^b	-46.23 ± 1.20	-53.8 ± 1.4^a	-25
Sr^{2+}		5.35 ± 0.07^a	-30.48 ± 1.28	-37.6 ± 0.3^a	-24
Ba^{2+}		4.34 ± 0.02^a	-24.80 ± 1.01	-29.6 ± 1.3^a	-16
Pb^{2+}		7.39 ± 0.11^a	-42.18 ± 1.11	-59.7 ± 1.2^a	-59
Cd^{2+}		4.08 ± 0.05^c	-23.29 ± 0.95	-22.4 ± 0.5^c	3
Hg^{2+}		3.69 ± 0.03^c	-21.01 ± 0.85	-21.1 ± 0.4^c	-0.3
	2	$\log K_s$	$\Delta_c G^\circ/\text{kJ}\cdot\text{mol}^{-1}$	$\Delta_c H^\circ/\text{kJ}\cdot\text{mol}^{-1}$	$\Delta_c S^\circ/\text{J}\cdot\text{K}^{-1}\cdot\text{mol}^{-1}$
Mg^{2+}		3.33 ± 0.05^c	-19.01 ± 1.10	$+48.1 \pm 0.8^c$	225
Ca^{2+}		12.16 ± 0.07^b	-69.41 ± 1.22	-65.3 ± 1.7^b	14
Sr^{2+}		7.90 ± 0.06^d	-45.10 ± 1.30	-49.8 ± 0.48^d	-16
Ba^{2+}		5.14 ± 0.02^a	-29.34 ± 0.40	-36.9 ± 0.8^a	-25
Pb^{2+}		9.30 ± 0.20^b	-53.09 ± 0.21	-62.7 ± 1.0^a	-32
Cd^{2+}		6.60 ± 0.10^c	-37.67 ± 1.07	-22.7 ± 0.6^c	50
Hg^{2+}		5.90 ± 0.20^d	-33.68 ± 1.40	-32.3 ± 0.9^d	5

^a Direct macrocalorimetry. ^b Competitive macrocalorimetry. ^c Direct microcalorimetry. ^d Competitive microcalorimetry titrations.

For systems with stability constants lower than 10^6 ($\log K_s = 6$), direct calorimetry (macro and micro) was the methodology used to derive $\log K_s$ (hence $\Delta_c G^\circ$) and $\Delta_c H^\circ$. Entropies of complexation were calculated from the relationship

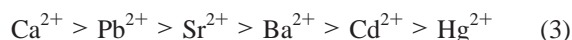
$$\Delta_c G^\circ = \Delta_c H^\circ - T\Delta_c S^\circ \quad (2)$$

For highly stable complexes ($\log K_s > 6$), competitive calorimetry was the technique selected. Thus, approximate $\log K_s$ value previously reported for Ca^{2+} and **1** in acetonitrile⁸ (determined by direct calorimetry) was accurately measured by this technique.

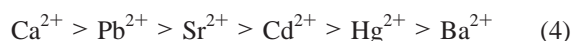
At this stage, it is relevant to discuss the role of the solvent in the complexation process (eq 1) although this will not alter the mathematical model used to derive the thermodynamic data. It may be correctly argued that thermodynamics does not provide structural information. On the other hand, it is indisputable that any model proposed must fit the experimental thermodynamic data and this is indeed the case for these systems.

On the basis of the downfield shift change observed for the aromatic protons in the ^1H NMR spectrum of **1** in CD_3CN relative to CDCl_3 , we have previously suggested^{10,33} that acetonitrile may be sitting in the hydrophobic cavity of the ligand and, as a result, the hydrophilic cavity of **1** is better preorganized to interact with univalent (mainly alkali-metal cations) in this solvent relative to methanol and benzonitrile. In fact, ^1H NMR studies in CD_3CN and CDCl_3 carried out for **2** show that the downfield shift for the aromatic protons in the former relative to the latter solvent are even more pronounced for this ligand ($\Delta\delta = 0.35$ ppm) than for **1** ($\Delta\delta = 0.25$ ppm). This interaction is concomitant with the X-ray structure of **2** that shows an acetonitrile molecule in its hydrophobic cavity with the nitrogen atom pointing away from the cavity.³⁴ These facts together with the lack of complexation observed for these ligands and bivalent cations in solvents (MeOH, DMF, PhCN) other than acetonitrile are strong indications that acetonitrile is sequestered in the hydrophobic cavity of these ligands not only in the solid state but also in solution. If so, the complexation of **1** and **2** with bivalent cations may involve the ligand-solvent adducts rather than the free ligands.

Furthermore, stability constant data shown in Table 5 are indicative that the interaction of these species with bivalent cations is selective. Thus for **1**, $\log K_s$ values follows that sequence,



while the sequence observed for ligand **2** is slightly altered for Ba^{2+} as shown below:

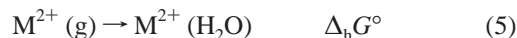


In thermodynamic terms, selectivity can be quantitatively assessed by the ratio of the stability constant for one cation over another. Thus, considering $K_{s(\text{Ca}^{2+})}/K_{s(\text{M}^{2+})}$, **1** is more selective for Ca^{2+} relative to Pb^{2+} , Sr^{2+} , Ba^{2+} , Cd^{2+} , and Hg^{2+} by factors of 6, 6.3×10^2 , 6.45×10^3 , 1.17×10^4 , and 2.88×10^4 , respectively, while for **2** the selectivity for Ca^{2+} relative to Pb^{2+} , Sr^{2+} , Cd^{2+} , Hg^{2+} , Ba^{2+} , and Mg^{2+} is higher by factors of 7.22×10^2 , 1.81×10^4 , 3.62×10^5 , 1.81×10^6 , 1.04×10^7 , and 6.74×10^8 , respectively.

Cation desolvation and ligand binding energy play a predominant role on the stability of complex formation of macrocycles and metal cations.³⁵ It is indeed the balance between these two processes, which contribute significantly to the equilibrium represented by eq 1. It is well established that while hydration (or solvation) energies for alkaline-earth metal cations are correlated with the electrostatic energies (z^2/r , where z is the cation charge and r is the ionic radius), there are some additional factors for the first transition and soft metal cations such as Hg^{2+} and Cd^{2+} (highly polarizable).³⁵ Therefore, it would not be useful to attempt to correlate $\Delta_c G^\circ$ values with the ionic radii. A more relevant parameter to consider would be their solvation Gibbs energies, $\Delta_{\text{solv}} G^\circ$.

There are few data on $\Delta_{\text{solv}} G^\circ$ values for bivalent cations in acetonitrile.³⁶ However, these data allow some approximations to be made to assess the predominant role either of the binding or the solvation energy on the complexation Gibbs energies of **1** and **2** and bivalent cations in acetonitrile. Considering that,

(i) $\Delta_{\text{solv}} G^\circ$ is made by the contribution of the hydration Gibbs energy, $\Delta_{\text{h}} G^\circ$, values (eq 5) and the transfer Gibbs energy, $\Delta_{\text{t}} G^\circ$ (eq 6) (data based on the $\text{Ph}_4\text{AsPh}_4\text{B}$ convention).³⁷



(ii) the $\Delta_{\text{t}} G^\circ$ values from water to acetonitrile ($\text{Ba}^{2+} = 57.3$ $\text{kJ}\cdot\text{mol}^{-1}$, $\text{Cd}^{2+} = 43.2$ $\text{kJ}\cdot\text{mol}^{-1}$)³⁶ are small relative to $\Delta_{\text{h}} G^\circ$ values ($\text{Ba}^{2+} = -1318$ $\text{kJ}\cdot\text{mol}^{-1}$, $\text{Cd}^{2+} = -1801$ $\text{kJ}\cdot\text{mol}^{-1}$),³⁶ and these do not alter the relative sequence for cations but makes $\Delta_{\text{solv}} G^\circ$ in MeCN slightly more positive than $\Delta_{\text{h}} G^\circ$; attempts are made to correlate $\Delta_c G^\circ$ with $\Delta_{\text{h}} G^\circ$ values. Thus, $\Delta_c G^\circ$ values for **1** and **2** and bivalent cations in acetonitrile are plotted against $\Delta_{\text{h}} G^\circ$ for these cations as shown in Figure 9.

This figure illustrates that these two forces (binding and desolvation) are partially compensated showing a selectivity peak. Thus, as far as Sr^{2+} , Ba^{2+} , Pb^{2+} , and Ca^{2+} cations are concerned, the absolute binding energy overcomes the increased energy required for the desolvation process. A maximum stability is reached for calcium, after which the binding energy is not enough to counteract the energetic requirements for cation desolvation. As a result, the stability decreases ($\Delta_c G^\circ$ becomes more positive) to an extent that relatively weak complexes, particularly for **1**, are found for magnesium (highest solvated cation) and these ligands in this solvent. No complexation was found between these ligands and the first transition-metal cations (Co^{2+} , Ni^{2+} , Cu^{2+} , and Zn^{2+}) in acetonitrile. Although this is predictable from the solvation energies of these cations, the nature of the donor atoms and their arrangement in the ligand structure are important factors in a complexation process involving these cations. Another important feature of Figure 9 is that absolute binding energies are in all cases higher for complexation processes involving **2** relative to **1**. Thus, the ligand effect on the complexation process (eq 1) can be assessed quantitatively in terms of their selectivity for a given cation relative to another in acetonitrile by considering the stability constant ratio ($K_{s(\text{M}^{2+}, \text{2})}/K_{s(\text{M}^{2+}, \text{1})}$). Thus, **2** is more selective than **1** by factors of 1.02×10^4 , 3.55×10^2 , 6.30 , 8.10×10^1 , 3.31×10^2 , and 1.62×10^2 for Ca^{2+} , Sr^{2+} , Ba^{2+} , Pb^{2+} , Cd^{2+} , and Hg^{2+} , respectively.

In an attempt to assess whether the selectivity peak observed in terms of Gibbs energies is enthalpy or entropy controlled, we consider the solvation enthalpies of bivalent cations in acetonitrile which are known for a few cations,³⁷ and these differ only slightly from hydration enthalpies. On these bases, the latter were used to establish whether a correlation is found between these data and the $\Delta_c H^\circ$ values reported in Table 5 for these ligands. Thus, a plot of $\Delta_c H^\circ$ against $\Delta_{\text{h}} H^\circ$ (Figure 10) shows a pattern similar to that observed for the Gibbs energies (Figure 9), except for **1** where the exothermic maximum is found for Pb^{2+} rather than for Ca^{2+} . Therefore, it is concluded that the

(33) Danil de Namor, A. F.; Apaza de Sueros, N.; McKervey, M. A.; Barrett, G.; Arnaud-Neu, F. A.; Schwing-Weill, M. J. *J. Chem. Soc., Chem. Comm.* **1991**, 1546.

(34) Danil de Namor, A. F.; Castellano, E. E.; Baron, K.; Piro, O. E., to be submitted for publication, 2002.

(35) Cox, B. G.; Schneider, H. *Coordination and Transport Properties of Macrocyclic Compounds in Solution*; Elsevier: New York, 1992.

(36) Burgess, J. *Metal Ion in Solution*; Ellis Horwood Limited: U.K., 1978.

(37) Cox, B. G.; Hedwig, G. R.; Parker, A. J.; Watts, D. W. *Aust. J. Chem.* **1974**, *27*, 477.

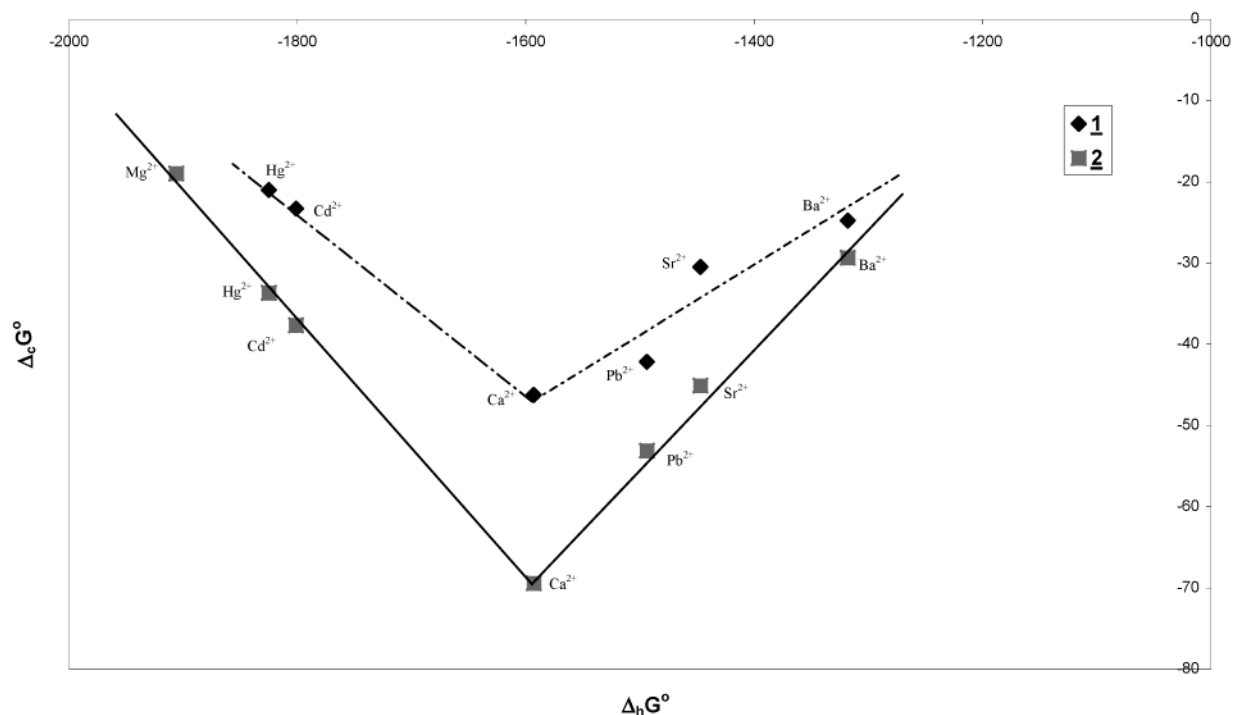


Figure 9. $\Delta_c G^\circ$ values for **1** and **2** against $\Delta_h G^\circ$ of bivalent metal cations in acetonitrile.

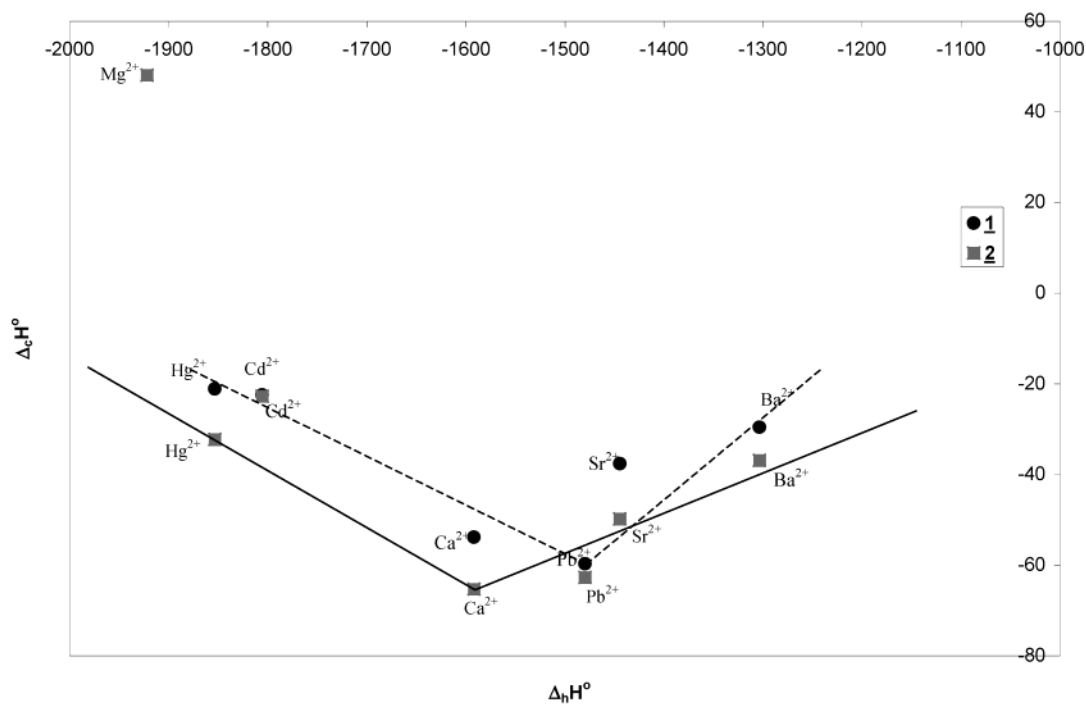


Figure 10. $\Delta_c H^\circ$ values for **1** and **2** against $\Delta_h H^\circ$ of bivalent metal cations in acetonitrile.

complexation process involving these ligands and bivalent cations is enthalpy controlled except for Mg^{2+} where the complexation process is entropy controlled. This may be attributed to the higher desolvation energy of the cation upon complexation. This statement is supported by the unfavorable enthalpy and the very favorable entropy observed for Mg^{2+} with the present calixarene ligands in acetonitrile solution.

Final Conclusions. From the above discussion, it is concluded that this paper demonstrates for the first time the following:

(i) The presence of acetonitrile leads to ligand's preorganization. This is illustrated by the major enhancement observed in complex stability with bivalent cations in this solvent relative to others (methanol, *N,N*-dimethylformamide, and benzonitrile) in which no complexation with these cations appears to occur.

(ii) These ligands discriminate between the various bivalent cations to the extent that a "selectivity" peak is found in terms of Gibbs energies when complexation data are plotted against cation solvation (hydration). Gibbs energies are in most cases mirrored by enthalpies and, therefore, for most cations (except

Mg²⁺) the process is enthalpy controlled. The selectivity peak observed is explained in terms of cation desolvation and binding.

(iii) The X-ray crystal structures of the cadmium and the lead complexes with the neutral guest show the versatile behavior of acetonitrile in the solid state.

Acknowledgment. Thanks are due to the European Commission for the financial support provided under contract ICA3 – CT – 2000 – 30006, FAPESP and CNPq (Brazil) and CONICET (Argentina).

Supporting Information Available: Tables of atomic coordinates and equivalent isotropic displacement parameters for complexes **3–6** (Tables S6–S9), corresponding full intramolecular bond distances and angles (Tables S10–S13), atomic anisotropic displacement parameters (Tables S14–S17), and hydrogen atoms positions (Tables S18–S21). An X-ray crystallographic file (CIF). This material is available free of charge via the Internet at <http://pubs.acs.org>.

JA020764+